ACS APPLIED MATERIALS & INTERFACES

Research Article

www.acsami.org

Toward Paper-Based Sensors: Turning Electrical Signals into an Optical Readout System

Devi D. Liana,[†,‡] Burkhard Raguse,[†] J. Justin Gooding,[‡,§] and Edith Chow*[,†]

[†]CSIRO Manufacturing Flagship, P. O. Box 218, Lindfield, New South Wales 2070, Australia

[‡]School of Chemistry, The University of New South Wales, Sydney, New South Wales 2052, Australia

[§]Australian Centre for NanoMedicine, The University of New South Wales, Sydney, New South Wales 2052, Australia

Supporting Information

ABSTRACT: Paper-based sensors are gaining increasing attention for their potential applications in resource-limited settings and for point-of-care analysis. However, chemical analysis of paper-based electronic sensors is frequently interpreted using complex software and electronic displays which compromise the advantages of using paper. In this work, we present two semiquantitative paper-based readout systems that can visually measure a change in resistance of a resistive-based sensor. The readout systems use electrochromic Prussian blue/polyaniline as an electrochromic indicator on a resistive gold nanoparticle film that is fabricated on paper. When the readout system is integrated with a resistive sensor in an electrical circuit, and a voltage is applied, the voltage drop along the readout system varies depending on the sensor's resistance. Due to the voltage gradient formed along the gold nanoparticle film, the overlaying Prussian blue/polyaniline will change color at voltages greater than its reduction voltage (green/blue for oxidized state and transparent for reduced state). Thus, the changes in resistances of a sensor can be semiquantified through color visualization by either measuring the length of the transparent film (analog readout system) or by counting the number of transparent segments (digital readout system). The work presented herein can potentially serve as an alternative paper-based display system for resistive sensors in instances where cost and weight is a premium.

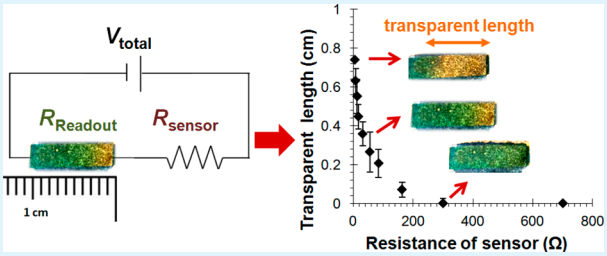

KEYWORDS: *paper-based sensor, electrochromic, readout system, colorimetric, display, gold nanoparticles, polyaniline, resistance*

1. INTRODUCTION

There has been growing interest in developing simple and low-cost devices where a yes/no answer or semiquantitative reading will suffice.[1,2] By eliminating the complexity in operation and rigorous analysis of data, wider acceptance and adoption of these device technologies will occur. Such devices may be suited for deployment in remote communities where access to laboratory infrastructure may be limited/costly, for patient or elderly healthcare monitoring in the home, or for direct in-field environmental monitoring.[1−4] These devices may allow the user (e.g., nurse, elderly person, and industrial worker) to perform the measurement with minimal user intervention as opposed to the expensive and sophisticated detection instrumentation which require operation by trained personnel.

Paper-based sensors[5−12] represent one such class of viable devices since paper is abundant, lightweight, biodegradable, and inexpensive. Developing a sensor from paper can be achieved through simple and cost-effective fabrication processes that are familiar to everyone such as printing, drawing, patterning, folding, and cutting.[10−12] Moreover, the paper substrate can be functionalized to change properties such as hydrophobicity, reactivity, and permeability to meet the user's requirement.[10−13] Paper also allows liquid transport through its hydrophilic matrix without the aid of external forces which is a property that Martinez et al.[14] exploited in the development of colorimetric bioassays on paper. Microfluidic channels were created from photoresist to define the reaction zones where each zone contained reagents for glucose and protein assays. A positive result was based on a change in color when an artificial urine sample spiked with the analytes of interest were spotted on paper and delivered to the reaction zones via capillary action. The work by Martinez et al. generated a lot of interest and subsequent research[15−33] since it demonstrated that paper could potentially be used as an inexpensive, portable substrate in remote settings.

Colorimetric detection has been widely used with paper-based sensors as a change in color or color intensity due to chemical or enzymatic interactions can be visually interpreted without any additional optical or electronic readout system.[17,32,34−42] Although simple, these colorimetric sensors are typically qualitative or semiquantitative. Paper-based sensors utilizing electrochemical transduction methods (voltammetric, amperometric, or conductometric)[16,18,20,25,43−45] have also been demonstrated and are generally more sensitive but rely

Received: June 5, 2015
Accepted: August 11, 2015
Published: August 19, 2015

DOI: 10.1021/acsami.5b04941
ACS Appl. Mater. Interfaces 2015, 7, 19201−19209

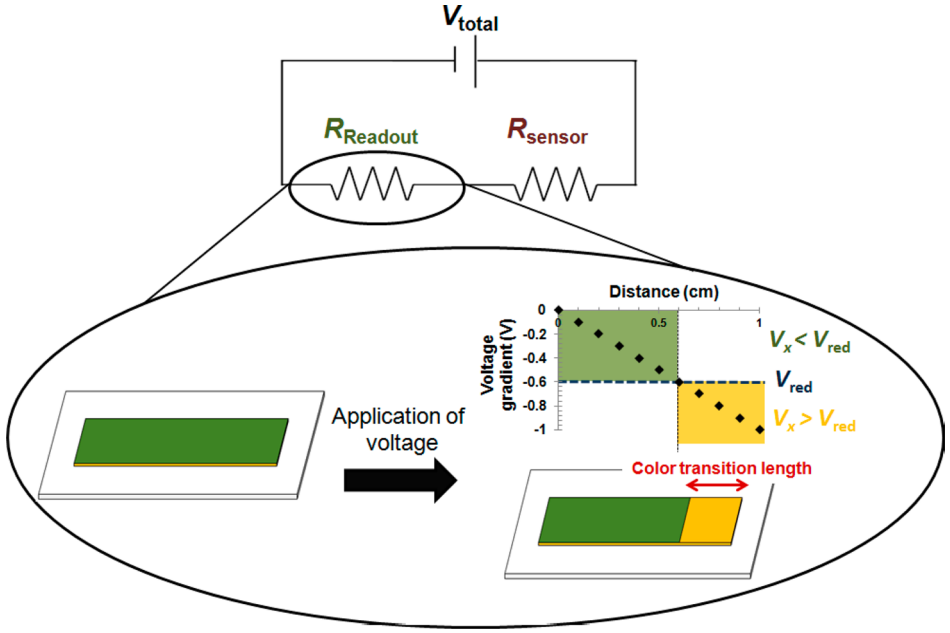

Figure 1. Basic operating principle of the paper-based readout system integrated with a sensor. The paper-based readout system consists of a resistive material ($R_{readout}$) coated with an electrochromic material. When a voltage is applied (V_{total}), then depending on the sensor's resistance (R_{sensor}), the electrochromic material on the readout system undergoes a color change at positions along the readout system where the voltage (V_x) is greater than the reduction voltage of the electrochromic material (V_{red}).

on expensive external electronics (e.g., a potentiostat and a computer system) to supply the power and display the result, which compromises the advantages of paper. Recently, smartphones have been used to display the readout and provide the power source in place of a potentiostat.[46−48] By connecting the paper-based sensor to the phone via the audio socket and playing an appropriate sound file, electrochemical reactions on the paper-based sensor can be initiated and the output signal can be analyzed using a custom written mobile phone application.[47] As powerful as this approach is, there are also applications that are incompatible with phones, for example, when weight is a premium, in resource-poor settings, or where the device is to be incorporated into clothing or bandages.

If all of the components of the device (sensor, power, and readout system) can be made on paper, then this will be a step toward a system that is truly paper-based. Liu and Crooks[49] developed an electrochemical sensing platform on paper with a metal/air battery as the power source and an electrochromic display. A piece of paper was used for liquid transport to bridge the battery, the electrochemical sensor, and display. Electrical contact was made to the paper through indium tin oxide electrodes. Upon introduction of artificial urine on paper, the metal/air battery was activated which drove electrocatalytic reactions of the analytes glucose and hydrogen peroxide. This resulted in a Prussian blue color change to Prussian white which could be correlated to the amount of glucose and hydrogen peroxide. Although not strictly all-paper-based, Liu and Crooks have successfully replaced the current signal that is usually generated from an electrochemical sensor into color visualization and have integrated the power source onto paper directly.

In order to extend the use of paper as a readout system, herein we demonstrate an electrochromic paper-based readout system that is suited for electrical resistance-based sensing. Resistance-based sensors (e.g., chemiresistors,[50−53] strain gauges,[54−56] and pressure sensors[57,58]) are widely used due to their simplicity and low-power operation and function by a change in electrical response due to chemical interaction or physical displacement. However, as discussed earlier, analysis of electrical and electrochemical signals is typically made through a computer or smartphone display. Our overall purpose is to develop an all-paper-based electronic device with the readout system presented here being the first step in that quest. The readout system will allow color visualization due to a change in the resistance of the sensor without the need for additional instrumentation. The main component of the readout system is a resistive material coated with an electrochromic species which is integrated in series with a resistive sensor in an electrical circuit (Figure 1). When a voltage (V_{total}) is applied to the circuit, the resistors (readout system and sensor) in the circuit will act as a voltage divider. Thus, the voltage drop across the sensor and the readout system will vary depending on the ratio of their resistances. For a readout system with a fixed resistance, $R_{readout}$, the voltage across the readout system will be affected by the value of R_{sensor}. Moreover, due to the generation of a linear voltage gradient along the resistive material of the system, the overlaying electrochromic material will be subjected to different voltages. Thus, the electrochromic material will change color at positions along the readout system where the voltage (V_x) is greater than the reduction voltage (V_{red}) of the electrochromic material. The length of the readout system that has changed color can then be measured and correlated with R_{sensor}.

As proof-of-concept, two semiquantitative paper-based readout systems using an electrochromic Prussian blue/polyaniline layer on top of a resistive thin film of gold nanoparticles are described herein. Both the electrical and chemical components of the readout system are fabricated directly on paper using simple drawing or brushing techniques. The reading is made by either (1) measuring the color transition length of the film (we refer to this as an analog readout system) or (2) counting the number of segments in the

DOI: 10.1021/acsami.5b04941
ACS Appl. Mater. Interfaces 2015, 7, 19201−19209

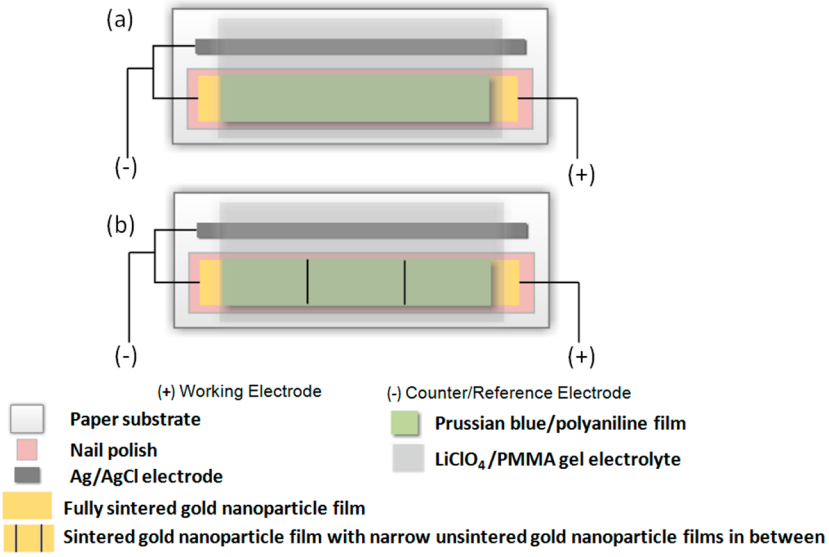

Figure 2. Schematic diagrams of an electrochromic paper-based (a) analog and (b) digital readout system. The analog readout system uses a fully sintered gold nanoparticle film as the working electrode whereas the digital readout system uses a number of sintered gold nanoparticle films with narrow unsintered gold nanoparticle films in between. The complete system consists of an electrochromic Prussian blue/polyaniline layer on top of the gold nanoparticle film and a Ag/AgCl electrode as the reference electrode. A $LiClO_4$/PMMA gel electrolyte covers both electrodes on the paper in order to assist the electron transfer between the two electrodes.

film that change color (we refer to this as a digital readout system). The readout system can measure changes in resistance of the sensor in an electrochromic manner without the need for an external electronic display. The work represents a step toward a low-cost, disposable paper-based readout system that can potentially be integrated with paper-based resistance sensors.

2. EXPERIMENTAL SECTION

2.1. Materials and Apparatus. All chemicals were of analytical grade, were used as received unless otherwise stated, and were purchased from Sigma-Aldrich (Sydney, Australia): hydrochloric acid, sodium dodecyl sulfate, propylene carbonate, acetonitrile, lithium perchlorate, poly(methyl methacrylate) (PMMA), potassium ferricyanide, tetraoctylammonium bromide (TOAB), toluene, sodium borohydride, sodium carbonate, hydrogen tetrachloroaurate, dimethylamino pyridine (DMAP), sulfuric acid, and 1-propanethiol. Aniline solution was purchased from BDH Chemicals Ltd., Radnor, PA, USA. Ferric chloride ($FeCl_3$) and ferric chloride hexahydrate ($FeCl_3{\cdot}6H_2O$) were from Ajax, Scoresby, Australia. All solutions were prepared in Milli-Q water (>18.2 MΩ cm from Millipore) unless otherwise stated. Ag/AgCl ink (AGCL−675 C) was purchased from Conductive Compounds, Hudson, NH, USA. Whatman filter paper (No. 1, 60 × 60 cm) was obtained from Sigma-Aldrich. Nail polish (satin sheet, Face of Australia) was purchased from Priceline (Sydney, Australia). A calligraphy pen (width 0.2 cm, Automatic Pen No. 1) was purchased from Will's Quills (Sydney, Australia).

2.2. Synthesis of Gold Nanoparticles Coated with DMAP. Gold nanoparticles were synthesized following the Brust method[59] and transferred to the aqueous phase using DMAP following the method by Gittins and Caruso.[60] The size of the DMAP-gold nanoparticles was 6 ± 2 nm, as determined by dynamic light scattering (high performance particle sizer, Malvern Instruments, Worcestershire, U.K.).

2.3. Synthesis of Polyaniline, Prussian Blue, and Gel Electrolyte. Polyaniline was chemically synthesized following the method by Kelly et al.[61] The as-synthesized polyaniline mixture in its emeraldine salt state was filtered, and the solid paste was collected prior to use. Prussian blue was prepared by mixing equal volumes of 40 mM $FeCl_3$ and 40 mM $K_3Fe(CN)_6$ in 10 mM HCl. A gel electrolyte was prepared by mixing 1 M $LiClO_4$ in propylene carbonate with 1.2 g of PMMA for 1 h at 130 °C.

2.4. Fabrication and Assembly of the Readout System. *2.4.1. General Fabrication.* A gold nanoparticle film was coated on paper using a technique described recently.[18] Briefly, ∼20 μL of 1.0% (w/v) DMAP-gold nanoparticles in 50% (v/v) ethanol was applied with a calligraphy pen (typical dimensions, 1−1.2 cm long and 0.2 cm wide) to paper coated with nail polish. Nail polish was applied to fill the pores of the paper such that the nanoparticle ink does not penetrate the paper. The paper was then transferred to a hot plate at 80 °C until the gold nanoparticle film dried and appeared golden (approximately 5 min). The typical resistance of a film was 10−12 MΩ. In order to reduce the resistance of the nanoparticle film to a suitable operating range, the film was subjected to a sintering process using a camera flash unit (Canon Speedlite 550 EX with Fresnel lens removed) positioned 1.1 cm away from the gold nanoparticle film (energy density of 2.1 J/cm^2).[18]

The electrochromic polyaniline and Prussian blue were applied on top of the fully sintered gold nanoparticle film by brushing approximately 0.8 mg of the polyaniline paste on top of the gold nanoparticle film followed by drying at 80 °C for 10 min on a hot plate. Subsequently, 10 μL of 40 mM Prussian blue solution was drop-cast on top of the polyaniline layer. After further drying at 80 °C for 10 min, the final film appeared green/blue. A reference electrode, Ag/AgCl ink, was painted (geometric area of 0.2 cm^2) adjacent to the gold nanoparticle film and connected to one end of the gold film. The reference electrode was used to facilitate a reversible redox reaction of Prussian blue/polyaniline. After the painting process, the ink was cured by placing the paper on the hot plate at 80 °C for 20 min. Both electrodes were then covered with a $LiClO_4$/PMMA gel electrolyte prior to measurement. The complete setup of the analog paper-based readout system is presented in Figure 2a.

2.4.2. Analog and Digital Readout System. The analog and digital readout systems differ in terms of the fabrication of the nanoparticle film component.

The analog paper-based readout system (Figure 2a) consists of a fully sintered gold nanoparticle film with a Prussian blue/polyaniline layer as described in the previous section. The resistance of a fully sintered gold nanoparticle film with Prussian blue/polyaniline layer was 10 ± 3 Ω (n = 5).

The digital paper-based readout system (Figure 2b) consists of a gold nanoparticle film with narrow unsintered gold nanoparticle films

DOI: 10.1021/acsami.5b04941
ACS Appl. Mater. Interfaces 2015, 7, 19201−19209

to serve as resistor between the sintered segments. The unsintered gold nanoparticle on the gold film were created by first printing an array of vertical lines (two, four, or nine lines, 0.05 cm wide) onto a transparency sheet using a SHARP MX-4111N printer (SHARP, Fyshwick, Australia) to form a mask. The patterned transparency sheet was then placed on top of the gold nanoparticle film prior to camera flash sintering. The gold nanoparticles that were covered by the black lines (width, 0.05 cm) remained unsintered and formed the resistive elements between the sintered segments. We varied the number of the narrow unsintered gold nanoparticles on the gold nanoparticle film from two, four, or nine lines resulting in three, five, or 10 sintered segments, respectively. After flash sintering, the resistance of the gold nanoparticle films having two, four, and nine resistive elements were 0.31 ± 0.08, 0.96 ± 0.22, and 2.11 ± 0.92 MΩ, respectively (n = 5). These films were then subjected to 1-propanethiol vapor exchange process to further reduce the resistance by hanging the film inside a 50 mL Schott bottle that was filled with 15 mL of 1-propanethiol solution for 1 h. Following this process, the electrochromic polyaniline and Prussian blue were applied along the entire gold nanoparticle film. The final resistances of the gold nanoparticle films with two, four, and nine resistive elements after application of Prussian blue/polyaniline were 18 ± 7, 23 ± 5, and 52 ± 11 Ω, respectively (n = 5).

2.5. Electrochemical Testing of the Readout System. To test the performance of the readout system, the two ends of the gold nanoparticle film were first connected to a potentiostat (PARSTAT 2273 Advanced Electrochemical System, Princeton Applied Research, Oak Ridge, TN, United States). The Ag/AgCl electrode was connected together with one end of the gold nanoparticle film (at the negative terminal) such that the potential at the Ag/AgCl electrode is the same as that end of the gold nanoparticle film. Thus, when a voltage difference is applied to the two ends of the gold nanoparticle film, a voltage gradient is generated along the film.

The voltage gradient along the gold nanoparticle film was measured after applying −1 V along the film using a Fluke 114 digital multimeter by placing one probe of the multimeter at one end of the gold nanoparticle film (negative terminal) while moving the other probe away at increments of 0.1 cm toward the other end of the gold nanoparticle film (positive terminal).

The readout system was characterized by applying a constant voltage along the readout system ($V_{readout}$) at values between 0 and −2.5 V. The transparent length was measured directly by drawing a scale adjacent to the film (for the analog readout system) or counting the number of segments that became transparent (for the digital readout system). Alternatively, for the analog readout system, the transparent length can be measured by taking an image of the readout system using a camera phone. The image was then analyzed using ImageJ software by converting the image into gray scale. By using the plot profile option, the color intensity profile along the film was obtained. The position where the color change started to occur was identified at 100 gray scale value and measured.

2.6. Integration of Readout System with a Model Sensor. In order to show that the readout system can measure changes in the resistance of a sensor, the readout system was connected in series to a resistor, R_{sensor}, as a model of a resistive-based sensor. The basic schematic shown in Figure 1 was also modified to include a variable resistor $R_{variable}$ connected in parallel to the model sensor. $R_{variable}$ (50 and 220 Ω for the analog and digital circuits, respectively) was used in order to increase the dynamic readout range of the sensor. The position at which the Prussian blue/polyaniline film changes color was measured and correlated with the resistance of the sensor.

2.7. Characterization of the Readout System. *2.7.1. Electrochromism of Prussian Blue/Polyaniline.* The coloration of Prussian blue/polyaniline was investigated using chronoamperometry by holding the potential at values of 0 to −2.0 V at a Prussian blue/polyaniline gold nanoparticle working electrode relative to a Ag/AgCl reference electrode in $LiClO_4$/PMMA gel electrolyte (see Supporting Information). The reduction voltage (V_{red}) of Prussian blue/polyaniline was identified.

2.7.2. Characterization of Gold Nanoparticle Film (Digital Readout System). In order to investigate whether the DMAP molecule that coated the unsintered gold nanoparticle film had been replaced with propanethiol, a Raman microscopy system equipped with a 633 nm laser (Renishaw Plc., Gloucestershire, U.K.) was used to measure the nanoparticle film before and after the propanethiol exchange process.

3. RESULTS AND DISCUSSION

3.1. Working Principle of the Electrochromic Readout System. Recording electrochemical/electrical signals from a sensor is commonly achieved using specific electronics plus associated software. However, to maintain the low cost of paper-based sensors, the choice of readout display needs to be reconsidered. Here, we demonstrate two readout systems that measure a change in the electrical potential of a resistance-based sensor and translate the signal to color visualization. Thus, the resistance change of sensors can be determined without the need for additional external readout electronics.

Prussian blue and polyaniline were chosen since they offer color visualization to the reader based on the redox state of these electrochromic materials. The combination of the two electrochromic materials was found to enhance the overall color of the film since the redox reactions of polyaniline and Prussian blue both occur over a similar voltage range.[62,63] The redox reaction of Prussian blue/polyaniline has been proposed as follows:[64,65]

$$\underset{\text{Polyaniline (Emeraldine salt)}}{(PANI^{2+})(ClO_4^-)_2} + \underset{\text{Prussian blue}}{Fe_4^{III}[Fe^{II}(CN)_6]_3} \underset{\text{Ox}}{\overset{\text{Red}}{\rightleftharpoons}} \underset{\text{Polyaniline (Leucoemeraldine)}}{PANI} + 2ClO_4^- + \underset{\text{Prussian white}}{Li_4Fe_4^{II}[Fe^{II}(CN)_6]_3} \quad (1)$$

Initially, the electrochromic behavior of Prussian blue/polyaniline layer was characterized by holding the potential of a Prussian blue/polyaniline/gold nanoparticle composite film at values between 0 and −2 V relative to Ag/AgCl (see the Supporting Information for more detail). The purpose was to ascertain the potential at which the Prussian blue/polyaniline changes color from green/blue (oxidized state) to transparent (reduced state) in the composite film system. It was shown (see Figure S1 in the Supporting Information) that the green/blue film of Prussian blue/polyaniline became transparent at a voltage of −0.6 V relative to Ag/AgCl. This voltage is denoted as V_{red} of the Prussian blue/polyaniline film.

In a similar manner, if a voltage is applied along the Prussian blue/polyaniline/gold nanoparticle composite film with the Ag/AgCl reference electrode being at the same potential as one end of the composite film as shown in Figure 2, then a voltage gradient will form along this composite film. For films which are uniform in resistance along the entire length, the voltage gradient along the film should be linear (see Figure 1). When a voltage exceeding V_{red} is applied along the composite film, a color change will be observed along parts of the film where the voltage V_x is greater than V_{red}. Due to the redox reaction being reversible, the Prussian blue/polyaniline will return to its initial state when the voltage is no longer applied. This is the basis for the electrochromic readout system described herein.

3.2. Analog Readout System. In the analog readout system, the resistive material consists entirely of a flash-sintered gold nanoparticle film with a resistance of 10 ± 3 Ω (n = 5). The uniformity of the sintering process should ensure a uniform electrical resistance along the film. Figure 3 shows the voltage gradient along the gold nanoparticle film when a constant voltage of −1 V was applied along the film (1.2 cm in length), and as expected, the voltage gradient was linear. As a result of the voltage gradient generated along the film, approximately 0.3 cm of the initial green/blue film of Prussian

DOI: 10.1021/acsami.5b04941
ACS Appl. Mater. Interfaces 2015, 7, 19201−19209

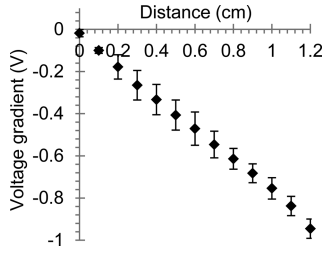

Figure 3. Voltage gradient along a 1.2 cm long Prussian blue/polyaniline gold nanoparticle film with a constant applied voltage of −1 V.

blue/polyaniline at the positive terminal became transparent within 30 s and did not change further with time (Figure 4a). The voltage (−0.7 V) determined at the position where Prussian blue/polyaniline became transparent is similar to the V_{red} value of Prussian blue/polyaniline of −0.6 V.

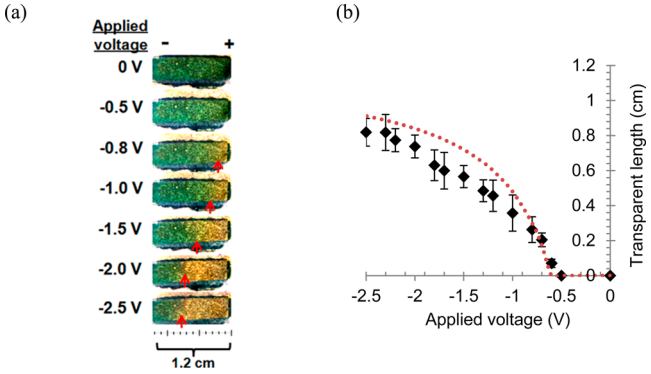

Figure 4. (a) Images of the Prussian blue/polyaniline gold nanoparticle film with different voltages applied along the gold nanoparticle film. The images were taken using a camera phone after 70 s of constant voltage application. The red arrow indicates where the transition of Prussian blue/polyaniline occurs. (b) Calibration curve showing the transparent length determined from ImageJ software at various applied voltages. The transparent length was measured relative to the positive terminal of the gold nanoparticle film. The data points and corresponding error bars reflect the average and standard deviation, respectively, of five composite films. The dotted line is the expected transparent length as a function of applied voltage.

The voltage applied along the Prussian blue/polyaniline/gold nanoparticle composite film was then varied between 0 and −2.5 V in order to observe how the transparent length changes with applied voltage (Figure 4a). When 0 and −0.5 V were applied, there was no discernible difference between the coloration of the readout system as the transition from green/blue to transparent only occurred at V_x greater than −0.6 V. As the voltage increased from −0.6 to −2.5 V there was a change in the transparent length as indicated by the red arrow in Figure 4a. Once again, the transition length closely corresponded to the expected values. Although the transition can be identified visually, a camera phone with ImageJ software was used to remove any subjective determination of where the color transition occurs. The length of the transparent film was then plotted against the applied voltage along the gold nanoparticle film (Figure 4b).

3.3. Digital Readout System. A digital readout system was developed by altering the resistive component of the readout system. Instead of using a gold nanoparticle film that is completely sintered, thus creating a linear voltage gradient with applied voltage, sintered gold nanoparticle films with a number of narrow unsintered gold nanoparticle films in between were formed. The narrow unsintered gold nanoparticle films serve as a higher resistive element that can increase the overall resistance of the readout system as well as provide segments with more abrupt voltage changes along the film. This can aid in the visualization of the readout system by having more discrete color changes and removing ambiguity as to exactly how far along the film the color change has occurred. To create regions of sintered and unsintered gold nanoparticle films, a straightforward method whereby regions that do not require sintering were covered with a photomask was used. This process eliminates the use of discrete resistors that are commonly used to increase the resistance in an electrical circuit. The digital readout system allows the user to count the number of sintered gold nanoparticle film segments that have become transparent after applying a constant voltage along the gold nanoparticle film.

To evaluate whether this approach is valid, we first formed a gold nanoparticle film with two narrow unsintered gold nanoparticle films (three sintered gold nanoparticle film segments), resulting in an overall film resistance of 313.8 ± 75 kΩ (n = 5). Note that the resistance of the films without the unsintered gold nanoparticle films was only of the order of 10 Ω as mentioned earlier. However, such a high resistance will not allow sufficient current to pass through the film for complete reduction of the Prussian blue/polyaniline layer to occur and be visualized. Thus, the resistance of the film was decreased through chemical modification. The film was first exposed to 1-propanethiol vapor for 1 h to exchange the DMAP coating on the nanoparticles with propanethiol, prior to coating the entire film with Prussian blue/polyaniline. It has been observed that interaction of polyaniline with thiolated-gold nanoparticles can cause a resistance decrease of the overall film.[66,67] Although the sintered nanoparticle film segments were also exposed to propanethiol, further reduction in resistance of these segments did not take place. Raman spectroscopy showed that the signature peak of DMAP molecules was absent in the gold nanoparticle film after flash sintering and vapor exchange with 1-propanethiol (see Figure S2 in the Supporting Information). After Prussian blue/polyaniline was applied on top of the gold nanoparticle film, the resistance decreased dramatically from approximately 300 kΩ to give a readout system resistance of 18 ± 7 Ω (see Figure S3 in the Supporting Information). The sheet resistance of the unsintered and sintered gold nanoparticle film was calculated to be 16 and 2.5 Ω/sq, respectively. This means that the narrow unsintered gold nanoparticle films serve as suitable higher resistive elements for the digital readout system.

Figure 5a illustrates how the voltage gradient varies along the gold nanoparticle film when −1 V was applied along either end. Instead of a linear voltage gradient along the film as for the analog readout system, the presence of the narrow unsintered gold nanoparticle films (located at positions indicated by the dashed lines on the graph) result in a steeper voltage drop along these regions. Figure 5b shows images of the digital readout system that were taken after 70 s of applying different voltages along the film. By counting the number of transparent sintered gold nanoparticle film segments, quantification is much simpler than for the analog readout system. However, the three-segment gold nanoparticle films demonstrated here is limited in its resolution.

DOI: 10.1021/acsami.5b04941
ACS Appl. Mater. Interfaces 2015, 7, 19201−19209

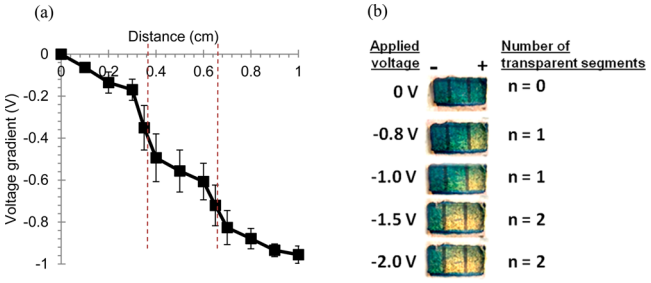

Figure 5. (a) Voltage gradient along a three-segment sintered gold nanoparticle film when a constant voltage of −1 V was applied. The dashed lines represent the positions where the unsintered gold nanoparticle films (0.05 cm in length) are located. (b) Images of the digital readout systems that were taken after 70 s of applying different constant voltages along the film.

To enable better resolution of the various applied voltages, the number of narrow unsintered gold nanoparticle films was increased to four (Figure 6a) and nine (Figure 6b) to result in

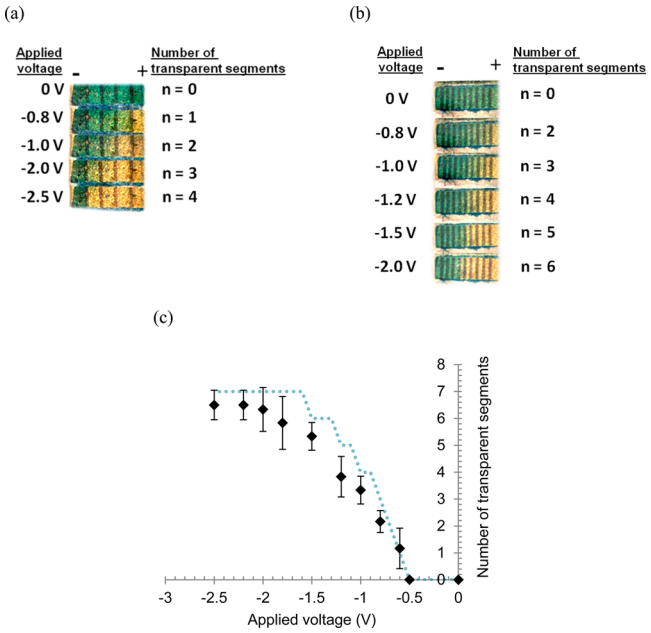

Figure 6. Images of a paper-based digital readout system with (a) five-segment sintered gold nanoparticle films and (b) 10-segment sintered gold nanoparticle films. (c) Plot of the number of sintered gold nanoparticle segments that became transparent upon application of different voltages along a digital readout system with a 10-segment sintered gold nanoparticle film. The data points and corresponding error bars reflect the average and standard deviation, respectively, of five composite films. The dotted line represents the calculated number of transparent segments as a function of applied voltage.

five-segment and 10-segment sintered gold nanoparticle films, respectively. As can be seen, increasing the number of narrow unsintered gold nanoparticle films allowed one to more clearly differentiate voltages along the readout system as well as identify smaller voltage changes. The individual sintered gold nanoparticle film segments are more uniform in color although there exist transition segments which are of low-intensity green/blue color. Figure 6c shows the number of transparent segments with applied voltage for a readout system with 10 sintered gold nanoparticle film segments.

3.4. Integration of the Paper-Based Readout System with a Model Sensor.

To demonstrate that the readout system can be used to determine the change in resistance of resistive sensors, these components were integrated in an electrical circuit. For proof-of-concept, a standard variable resistor was used as a model of the sensor (R_{sensor}) and was connected in series with the resistive readout system $R_{readout}$ (Figure 1). When a voltage (V_{total}) is applied to the circuit, the two resistors in the circuit act as a voltage divider:

$$\frac{V_{readout}}{V_{total}} = \frac{R_{readout}}{R_{readout} + R_{sensor}} \quad (2)$$

Rearranging eq 2 gives

$$R_{sensor} = \frac{(V_{total} - V_{readout})R_{readout}}{V_{readout}} \quad (3)$$

For the readout system to be applicable for the sensor, the voltage drop along the readout system needs to be in the range of −0.6 to −2.0 V where Prussian blue/polyaniline is in its transparent reduced state. From eq 3, with a total applied voltage of −3 V and using an analog readout system with $R_{readout}$ = 10 Ω, one can deduce that R_{sensor} should be in the range of 5−40 Ω for the condition −0.6 V < $V_{readout}$ < −2.0 V to be met. This is a very limited dynamic readout range for the sensor. In order to increase the dynamic readout range a variable resistor, $R_{variable}$, was placed in parallel to R_{sensor} to decrease the overall resistance of the two parallel resistors, $R_{sensor}//R_{variable}$, and thereby increase the voltage drop along the readout system. In the presence of $R_{variable}$:

$$\frac{V_{readout}}{V_{total}} = \frac{R_{readout}}{R_{readout} + R_{sensor} // R_{variable}} \quad (4)$$

where

$$R_{sensor} // R_{variable} = \frac{R_{sensor}R_{variable}}{R_{sensor} + R_{variable}}$$

Rearranging eq 4 gives

$$R_{sensor} = \frac{(V_{total} - V_{readout})R_{readout}R_{variable}}{(V_{readout}R_{readout} + V_{readout}R_{variable} - V_{total}R_{readout})} \quad (5)$$

With the incorporation of a variable resistor of 50 Ω, a total applied voltage of −3 V, and $R_{readout}$ of 10 Ω, the value of R_{sensor} should be in the range of 5−200 Ω for a reading to be interpreted. To verify this experimentally, we first set the resistance of R_{sensor} between 300 and 700 Ω. When a constant voltage of −3 V was applied to the circuit, the voltage along the analog readout system was less than −0.6 V. Such a voltage was not able to reduce the Prussian blue/polyaniline layer on the gold nanoparticle film. Thus, no transparent region on the gold nanoparticle film was visible. As the resistance of R_{sensor} was tuned to between 80 and 160 Ω, the voltage along the readout system encompassed the reduction voltage of Prussian blue/polyaniline. Hence, some regions of the gold nanoparticle film became transparent. When R_{sensor} was decreased even further to 6 Ω, 0.7 cm of the film became transparent. Figure 7a represents the transparent length as a function of the sensor's resistance. The results show that a resistance between 6 and 160 Ω can be semiquantitatively determined using the analog readout system.

DOI: 10.1021/acsami.5b04941
ACS Appl. Mater. Interfaces 2015, 7, 19201−19209

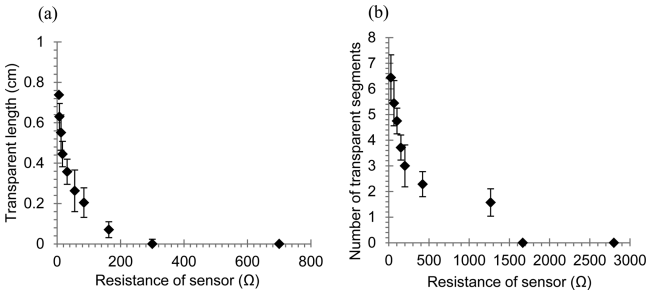

Figure 7. (a) Calibration curve of the analog readout system showing the relationship between the resistance of the model sensor and the length of the Prussian blue/polyaniline/gold nanoparticle film that is transparent. (b) Calibration curve of the digital readout system with a 10-segment sintered gold nanoparticle film showing the relationship between the resistance of the model sensor and the number of segments of the film that are transparent. In both cases the applied voltage was −3 V. The data points and corresponding error bars reflect the average and standard deviations, respectively, of five measurements.

An alternative method to increase the dynamic readout range of the sensor is to increase $R_{readout}$. In the analog readout system, $R_{readout}$ is 10 Ω, but for the digital readout system with the 10-segment sintered gold nanoparticle films $R_{readout}$ = 50 Ω. When the digital readout system was connected in series with the sensor, a reading could be interpreted for R_{sensor} in the range between 25 and 200 Ω. This is already a much better dynamic range than the 5−40 Ω that was calculated for the analog readout system with no variable resistor. When a variable resistor of 220 Ω was placed in parallel to the sensor, the resistance range of the model sensor that could be measured by the digital readout system was 30−1100 Ω (Figure 7b) which is within the calculated range of 28−2200 Ω. Thus, the incorporation of $R_{variable}$ to the circuit and a higher value of $R_{readout}$ improves the readable dynamic range of the sensor.

For the paper-based readout system to be truly compatible with resistive-based sensors, it needs to be able to not just determine the resistance of the sensor but also record changes in the resistance that may occur over time. Based on the results in Figure 7b for a digital readout system, changes in a sensor's resistance of over 50% can be measured from the readout system. This readout system would be suited for sensors that are highly sensitive to their chemical environment (chemiresistors[50−52]), mechanical forces (strain gauges[54,55,68]), and touch (pressure sensors[57,58]). It should be noted that although incorporating a variable resistor in parallel to a resistive sensor can increase the dynamic readout range of the sensor, this comes at a cost of sensitivity. For example when a variable resistor of 220 Ω is placed in parallel to a sensor of resistance 1100 Ω, the majority of the current will flow through the variable resistor rather than through the sensor. In effect, the current sensitivity to the resistive sensor component is being diminished. Thus, increasing the readable dynamic range by increasing the resistance of the readout system is a more practical solution than incorporating a variable resistor. On the other hand, since the sensors to be integrated will be electrical-resistance-based, it may be possible to tune the sensor's resistance to a range compatible with the readout system by altering the electrode spacing and area.

The readout systems presented here are proof-of-concept demonstrations that changes in electrical resistance values can be determined colorimetrically on paper. By increasing the resistance of the readout system further, it should be possible to increase the readable dynamic range of the sensor and improve the sensitivity of the readout system. Additionally, it should also be possible to tune the response of the readout system to different voltage range and colors by using other electrochromic redox materials.

4. CONCLUSIONS

We presented two semiquantitative paper-based readout systems that are capable of measuring changes in resistances in an electrochromic manner without the need for an external electronic display. The fabrication of the readout system was simple, requiring only drawing, brushing, drying, and camera flash sintering of the components on paper. By depositing Prussian blue/polyaniline on top of a resistive gold nanoparticle film, a color change along the film (from green/blue to transparent) occurred depending on the voltage along the film. The resultant voltage drop produced a change in the length of the transparent portion of the film (analog readout system) or the number of transparent segments (digital readout system). By integrating the resistive readout system with a model resistive sensor in an electrical circuit, changes in the resistance of the sensor could be deduced by interpreting color changes along the readout system. In a digital readout system, with a variable resistor in the circuit, resistance values of a model sensor in the range of 30−1100 Ω could be determined along with changes in resistance values of over 50%. We have successfully shown how the dynamic readout range can be tuned by varying the resistance of the readout system and the incorporation of a variable resistor in parallel to the sensor.

This work represents proof-of-concept studies of using a paper-based electrochromic readout system in conjunction with resistive-based sensors. It reveals promise for further development whereby the sensitivity and dynamic range can be tuned further and made useful for any of the classes of resistive-based sensors such as chemiresistors, strain gauges, or pressure sensors. In particular, the readout system is a suitable alternative to electronic screen displays for applications where low-cost and/or lightweight devices are imperative. The work presented here is a shift in focus from just sensing on paper to displaying the results from a sensing system on paper, which is a hurdle that needs to be overcome for paper-based devices to be truly compatible with real-world applications.

■ ASSOCIATED CONTENT

Supporting Information

The Supporting Information is available free of charge on the ACS Publications website at DOI: 10.1021/acsami.5b04941.

Characterization of the electrochromic properties of Prussian blue/polyaniline on gold nanoparticle film, characterization of the unsintered gold nanoparticle film, and the resistance effect of propanethiol coated gold nanoparticle films with polyaniline (PDF)

■ AUTHOR INFORMATION

Corresponding Author

*E-mail: edith.chow@csiro.au. Tel.: +61-2-9413-7062.

Notes

The authors declare no competing financial interest.

DOI: 10.1021/acsami.5b04941
ACS Appl. Mater. Interfaces 2015, 7, 19201−19209

■ ACKNOWLEDGMENTS

We thank J. Myers for her help in synthesizing the gold nanoparticles.

■ REFERENCES

(1) Peeling, R.; Mabey, D. Point-of-Care Tests for Diagnosing Infections in the Developing World. *Clin. Microbiol. Infect.* **2010**, *16*, 1062−1069.
(2) Price, C. P. Regular Review: Point of Care Testing. *BMJ.* **2001**, *322*, 1285−1288.
(3) Tüdős, A. J.; Besselink, G. A.; Schasfoort, R. B. Trends in Miniaturized Total Analysis Systems for Point-of-Care Testing in Clinical Chemistry. *Lab Chip* **2001**, *1*, 83−95.
(4) Ahn, C. H.; Choi, J. W.; Beaucage, G.; Nevin, J. H.; Lee, J. B.; Puntambekar, A.; Lee, J. Y. Disposable Smart Lab on a Chip for Point-of-Care Clinical Diagnostics. *Proc. IEEE* **2004**, *92*, 154−173.
(5) Liana, D. D.; Raguse, B.; Gooding, J. J.; Chow, E. Recent Advances in Paper-Based Sensors. *Sensors* **2012**, *12*, 11505−11526.
(6) Cate, D. M.; Adkins, J. A.; Mettakoonpitak, J.; Henry, C. S. Recent Developments in Paper-Based Microfluidic Devices. *Anal. Chem.* **2015**, *87*, 19−41.
(7) Hu, J.; Wang, S.; Wang, L.; Li, F.; Pingguan-Murphy, B.; Lu, T. J.; Xu, F. Advances in Paper-Based Point-of-Care Diagnostics. *Biosens. Bioelectron.* **2014**, *54*, 585−597.
(8) Li, X.; Ballerini, D. R.; Shen, W. A Perspective on Paper-Based Microfluidics: Current Status and Future Trends. *Biomicrofluidics* **2012**, *6*, 011301.
(9) Rozand, C. Paper-Based Analytical Devices for Point-of-Care Infectious Disease Testing. *Eur. J. Clin. Microbiol. Infect. Dis.* **2014**, *33*, 147−156.
(10) Nery, E. W.; Kubota, L. T. Sensing Approaches on Paper-Based Devices: A Review. *Anal. Bioanal. Chem.* **2013**, *405*, 7573−7595.
(11) Yetisen, A. K.; Akram, M. S.; Lowe, C. R. Paper-Based Microfluidic Point-of-Care Diagnostic Devices. *Lab Chip* **2013**, *13*, 2210−2251.
(12) Mahadeva, S. K.; Walus, K.; Stoeber, B. Paper as a Platform for Sensing Applications and Other Devices: A Review. *ACS Appl. Mater. Interfaces* **2015**, *7*, 8345−8362.
(13) Maxwell, E. J.; Mazzeo, A. D.; Whitesides, G. M. Paper-Based Electroanalytical Devices for Accessible Diagnostic Testing. *MRS Bull.* **2013**, *38*, 309−314.
(14) Martinez, A. W.; Phillips, S. T.; Butte, M. J.; Whitesides, G. M. Patterned Paper as a Platform for Inexpensive, Low-Volume, Portable Bioassays. *Angew. Chem., Int. Ed.* **2007**, *46*, 1318−1320.
(15) Martinez, A. W.; Phillips, S. T.; Whitesides, G. M.; Carrilho, E. Diagnostics for the Developing World: Microfluidic Paper-Based Analytical Devices. *Anal. Chem.* **2010**, *82*, 3−10.
(16) Dungchai, W.; Chailapakul, O.; Henry, C. S. Electrochemical Detection for Paper-Based Microfluidics. *Anal. Chem.* **2009**, *81*, 5821−5826.
(17) Lewis, G. G.; DiTucci, M. J.; Phillips, S. T. Quantifying Analytes in Paper-Based Microfluidic Devices Without Using External Electronic Readers. *Angew. Chem., Int. Ed.* **2012**, *51*, 12707−12710.
(18) Liana, D. D.; Raguse, B.; Wieczorek, L.; Baxter, G. R.; Chuah, K.; Gooding, J. J.; Chow, E. Sintered Gold Nanoparticles as an Electrode Material for Paper-Based Electrochemical Sensors. *RSC Adv.* **2013**, *3*, 8683−8691.
(19) Arena, A.; Donato, N.; Saitta, G.; Bonavita, A.; Rizzo, G.; Neri, G. Flexible Ethanol Sensors on Glossy Paper Substrates Operating at Room Temperature. *Sens. Actuators, B* **2010**, *145*, 488−494.
(20) Carvalhal, R. F.; Simão Kfouri, M.; de Oliveira Piazetta, M. H.; Gobbi, A. L.; Kubota, L. T. Electrochemical Detection in a Paper-Based Separation Device. *Anal. Chem.* **2010**, *82*, 1162−1165.
(21) Cheng, C. M.; Martinez, A. W.; Gong, J.; Mace, C. R.; Phillips, S. T.; Carrilho, E.; Mirica, K. A.; Whitesides, G. M. Paper-Based ELISA. *Angew. Chem., Int. Ed.* **2010**, *49*, 4771−4774.
(22) Delaney, J. L.; Hogan, C. F.; Tian, J.; Shen, W. Electrogenerated Chemiluminescence Detection in Paper-Based Microfluidic Sensors. *Anal. Chem.* **2011**, *83*, 1300−1306.
(23) Fenton, E. M.; Mascarenas, M. R.; López, G. P.; Sibbett, S. S. Multiplex Lateral-Flow Test Strips Fabricated by Two-Dimensional Shaping. *ACS Appl. Mater. Interfaces* **2009**, *1*, 124−129.
(24) Mazzeo, A. D.; Kalb, W. B.; Chan, L.; Killian, M. G.; Bloch, J. F.; Mazzeo, B. A.; Whitesides, G. M. Paper-Based, Capacitive Touch Pads. *Adv. Mater.* **2012**, *24*, 2850−2856.
(25) Nie, Z.; Nijhuis, C. A.; Gong, J.; Chen, X.; Kumachev, A.; Martinez, A. W.; Narovlyansky, M.; Whitesides, G. M. Electrochemical Sensing in Paper-Based Microfluidic Devices. *Lab Chip* **2010**, *10*, 477−483.
(26) Zhang, M.; Ge, L.; Ge, S.; Yan, M.; Yu, J.; Huang, J.; Liu, S. Three-Dimensional Paper-Based Electrochemiluminescence Device for Simultaneous Detection of Pb 2+ and Hg 2+ Based on Potential Control Technique. *Biosens. Bioelectron.* **2013**, *41*, 544−550.
(27) Wang, S.; Ge, L.; Song, X.; Yu, J.; Ge, S.; Huang, J.; Zeng, F. Paper-Based Chemiluminescence ELISA: Lab-on-Paper Based on Chitosan Modified Paper Device and Wax-Screen-Printing. *Biosens. Bioelectron.* **2012**, *31*, 212−218.
(28) Liu, H.; Crooks, R. M. Three-Dimensional Paper Microfluidic Devices Assembled Using the Principles of Origami. *J. Am. Chem. Soc.* **2011**, *133*, 17564−17566.
(29) Li, R. Z.; Hu, A.; Zhang, T.; Oakes, K. D. Direct Writing on Paper of Foldable Capacitive Touch Pads with Silver Nanowire Inks. *ACS Appl. Mater. Interfaces* **2014**, *6*, 21721−21729.
(30) Kumar, S.; Kaushik, S.; Pratap, R.; Raghavan, S. Graphene on Paper: A Simple, Low-Cost Chemical Sensing Platform. *ACS Appl. Mater. Interfaces* **2015**, *7*, 2189−2194.
(31) Li, L.; Huang, X.; Liu, W.; Shen, W. Control Performance of Paper-Based Blood Analysis Devices Through Paper Structure Design. *ACS Appl. Mater. Interfaces* **2014**, *6*, 21624−21631.
(32) Xu, M.; Bunes, B. R.; Zang, L. Paper-Based Vapor Detection of Hydrogen Peroxide: Colorimetric Sensing with Tunable Interface. *ACS Appl. Mater. Interfaces* **2011**, *3*, 642−647.
(33) Li, X.; Wang, Y.-H.; Zhao, C.; Liu, X. Paper-Based Piezoelectric Touch Pads with Hydrothermally Grown Zinc Oxide Nanowires. *ACS Appl. Mater. Interfaces* **2014**, *6*, 22004−22012.
(34) Dungchai, W.; Chailapakul, O.; Henry, C. S. Use of Multiple Colorimetric Indicators for Paper-Based Microfluidic Devices. *Anal. Chim. Acta* **2010**, *674*, 227−233.
(35) Martinez, A. W.; Phillips, S. T.; Carrilho, E.; Thomas, S. W., III; Sindi, H.; Whitesides, G. M. Simple Telemedicine for Developing Regions: Camera Phones and Paper-Based Microfluidic Devices for Real-Time, Off-Site Diagnosis. *Anal. Chem.* **2008**, *80*, 3699−3707.
(36) Zhao, W.; Ali, M. M.; Aguirre, S. D.; Brook, M. A.; Li, Y. Paper-Based Bioassays Using Gold Nanoparticle Colorimetric Probes. *Anal. Chem.* **2008**, *80*, 8431−8437.
(37) Jokerst, J. C.; Adkins, J. A.; Bisha, B.; Mentele, M. M.; Goodridge, L. D.; Henry, C. S. Development of a Paper-Based Analytical Device for Colorimetric Detection of Select Foodborne Pathogens. *Anal. Chem.* **2012**, *84*, 2900−2907.
(38) Coskun, A. F.; Wong, J.; Khodadadi, D.; Nagi, R.; Tey, A.; Ozcan, A. A Personalized Food Allergen Testing Platform on a Cellphone. *Lab Chip* **2013**, *13*, 636−640.
(39) Cretich, M.; Sedini, V.; Damin, F.; Pelliccia, M.; Sola, L.; Chiari, M. Coating of Nitrocellulose for Colorimetric DNA Microarrays. *Anal. Biochem.* **2010**, *397*, 84−88.
(40) Medley, C. D.; Smith, J. E.; Tang, Z.; Wu, Y.; Bamrungsap, S.; Tan, W. Gold Nanoparticle-Based Colorimetric Assay for the Direct Detection of Cancerous Cells. *Anal. Chem.* **2008**, *80*, 1067−1072.
(41) Wang, W.; Wu, W.-Y.; Wang, W.; Zhu, J.-J. Tree-Shaped Paper Strip for Semiquantitative Colorimetric Detection of Protein with Self-Calibration. *J. Chromatogr. A* **2010**, *1217*, 3896−3899.
(42) Cate, D. M.; Dungchai, W.; Cunningham, J. C.; Volckens, J.; Henry, C. S. Simple, Distance-Based Measurement for Paper Analytical Devices. *Lab Chip* **2013**, *13*, 2397−2404.

DOI: 10.1021/acsami.5b04941
ACS Appl. Mater. Interfaces 2015, 7, 19201−19209

(43) Tan, S. N.; Ge, L.; Tan, H. Y.; Loke, W. K.; Gao, J.; Wang, W. Paper-Based Enzyme Immobilization for Flow Injection Electrochemical Biosensor Integrated with Reagent-Loaded Cartridge Toward Portable Modular Device. *Anal. Chem.* **2012**, *84*, 10071−10076.
(44) Pozuelo, M.; Blondeau, P.; Novell, M.; Andrade, F. J.; Rius, F. X.; Riu, J. Paper-Based Chemiresistor for Detection of Ultralow Concentrations of Protein. *Biosens. Bioelectron.* **2013**, *49*, 462−465.
(45) Mirica, K. A.; Azzarelli, J. M.; Weis, J. G.; Schnorr, J. M.; Swager, T. M. Rapid Prototyping of Carbon-Based Chemiresistive Gas Sensors on Paper. *Proc. Natl. Acad. Sci. U. S. A.* **2013**, *110*, E3265−E3270.
(46) Mudanyali, O.; Dimitrov, S.; Sikora, U.; Padmanabhan, S.; Navruz, I.; Ozcan, A. Integrated Rapid-Diagnostic-Test Reader Platform on a Cellphone. *Lab Chip* **2012**, *12*, 2678−2686.
(47) Delaney, J. L.; Doeven, E. H.; Harsant, A. J.; Hogan, C. F. Use of a Mobile Phone for Potentiostatic Control with Low Cost Paper-Based Microfluidic Sensors. *Anal. Chim. Acta* **2013**, *790*, 56−60.
(48) Zhu, H.; Sencan, I.; Wong, J.; Dimitrov, S.; Tseng, D.; Nagashima, K.; Ozcan, A. Cost-Effective and Rapid Blood Analysis on a Cell-Phone. *Lab Chip* **2013**, *13*, 1282−1288.
(49) Liu, H.; Crooks, R. M. Paper-Based Electrochemical Sensing Platform with Integral Battery and Electrochromic Read-Out. *Anal. Chem.* **2012**, *84*, 2528−2532.
(50) Raguse, B.; Chow, E.; Barton, C. S.; Wieczorek, L. Gold Nanoparticle Chemiresistor Sensors: Direct Sensing of Organics in Aqueous Electrolyte Solution. *Anal. Chem.* **2007**, *79*, 7333−7339.
(51) Lai, L. M. H.; Goon, I. Y.; Chuah, K.; Lim, M.; Braet, F.; Amal, R.; Gooding, J. J. The Biochemiresistor: An Ultrasensitive Biosensor for Small Organic Molecules. *Angew. Chem., Int. Ed.* **2012**, *51*, 6456−6459.
(52) Cooper, J.; Kiiveri, H.; Hubble, L.; Chow, E.; Webster, M.; Müller, K.-H.; Sosa-Pintos, A.; Bendavid, A.; Raguse, B.; Wieczorek, L. Quantifying BTEX in Aqueous Solutions with Potentially Interfering Hydrocarbons Using a Partially Selective Sensor Array. *Analyst* **2015**, *140*, 3233−3238.
(53) Hubble, L. J.; Chow, E.; Cooper, J. S.; Webster, M.; Müller, K.-H.; Wieczorek, L.; Raguse, B. Gold Nanoparticle Chemiresistors Operating in Biological Fluids. *Lab Chip* **2012**, *12*, 3040−3048.
(54) Herrmann, J.; Müller, K.-H.; Reda, T.; Baxter, G.; Raguse, B.; De Groot, G.; Chai, R.; Roberts, M.; Wieczorek, L. Nanoparticle Films as Sensitive Strain Gauges. *Appl. Phys. Lett.* **2007**, *91*, 183105.
(55) Hu, N.; Karube, Y.; Yan, C.; Masuda, Z.; Fukunaga, H. Tunneling Effect in a Polymer/Carbon Nanotube Nanocomposite Strain Sensor. *Acta Mater.* **2008**, *56*, 2929−2936.
(56) Gullapalli, H.; Vemuru, V. S.; Kumar, A.; Botello-Mendez, A.; Vajtai, R.; Terrones, M.; Nagarajaiah, S.; Ajayan, P. M. Flexible Piezoelectric ZnO−Paper Nanocomposite Strain Sensor. *Small* **2010**, *6*, 1641−1646.
(57) Lipomi, D. J.; Vosgueritchian, M.; Tee, B. C.; Hellstrom, S. L.; Lee, J. A.; Fox, C. H.; Bao, Z. Skin-Like Pressure and Strain Sensors Based on Transparent Elastic Films of Carbon Nanotubes. *Nat. Nanotechnol.* **2011**, *6*, 788−792.
(58) Saito, M.; Nakajima, K.; Takano, C.; Ohta, Y.; Sugimoto, C.; Ezoe, R.; Sasaki, K.; Hosaka, H.; Ifukube, T.; Ino, S.; Yamashita, K. An In-Shoe Device to Measure Plantar Pressure During Daily Human Activity. *Med. Eng. Phys.* **2011**, *33*, 638−645.
(59) Brust, M.; Walker, M.; Bethell, D.; Schiffrin, D. J.; Whyman, R. Synthesis of Thiol-Derivatised Gold Nanoparticles in a Two-Phase Liquid−Liquid System. *J. Chem. Soc., Chem. Commun.* **1994**, 801−802.
(60) Gittins, D. I.; Caruso, F. Spontaneous Phase Transfer of Nanoparticulate Metals from Organic to Aqueous Media. *Angew. Chem., Int. Ed.* **2001**, *40*, 3001−3004.
(61) Kelly, F. M.; Meunier, L.; Cochrane, C.; Koncar, V. Polyaniline: Application as Solid State Electrochromic in a Flexible Textile Display. *Displays* **2013**, *34*, 1−7.
(62) Jelle, B. P.; Hagen, G. Electrochemical Multilayer Deposition of Polyaniline and Prussian Blue and Their Application in Solid State Electrochromic Windows. *J. Appl. Electrochem.* **1998**, *28*, 1061−1065.
(63) DeLongchamp, D. M.; Hammond, P. T. Multiple-Color Electrochromism from Layer-By-Layer-Assembled Polyaniline/Prussian Blue Nanocomposite Thin Films. *Chem. Mater.* **2004**, *16*, 4799−4805.
(64) Leventis, N.; Chung, Y. C. Polyaniline-Prussian Blue Novel Composite Material for Electrochromic Applications. *J. Electrochem. Soc.* **1990**, *137*, 3321−3322.
(65) Hong, S. F.; Hwang, S. C.; Chen, L. C. Deposition-Order-Dependent Polyelectrochromic and Redox Behaviors of the Polyaniline−Prussian Blue Bilayer. *Electrochim. Acta* **2008**, *53*, 6215−6227.
(66) Shirsat, M. D.; Bangar, M. A.; Deshusses, M. A.; Myung, N. V.; Mulchandani, A. Polyaniline Nanowires-Gold Nanoparticles Hybrid Network Based Chemiresistive Hydrogen Sulfide Sensor. *Appl. Phys. Lett.* **2009**, *94*, 083502.
(67) Yoo, K. S.; Sorensen, I. W.; Glaunsinger, W. S. Adhesion, Surface Morphology, and Gas Sensing Characteristics of Thin-Gold-Film Chemical Sensors. *J. Vac. Sci. Technol., A* **1994**, *12*, 192−198.
(68) Mattmann, C.; Clemens, F.; Tröster, G. Sensor for Measuring Strain in Textile. *Sensors* **2008**, *8*, 3719−3732.

DOI: 10.1021/acsami.5b04941
ACS Appl. Mater. Interfaces 2015, 7, 19201−19209